Analytical Event Count Prediction in Monotonic Event-Triggered Control Systems

Karel Walter Gomez Orellana
Independent Researcher
La Paz, Bolivia
karelgomez124@ieee.org

Cristhian Joel Apaza Flores
Ingeniería Electrónica
Universidad Mayor de San Andrés
La Paz, Bolivia
crissapazaf@gmail.com

Jorge Antonio Nava Amador
Ingeniería Electrónica
Universidad Mayor de San Andrés
La Paz, Bolivia
janava@umsa.bo

***Abstract*—This paper presents an analytical framework for event-triggered control (ETC) in linear time-invariant (LTI) systems exhibiting monotonic step responses. We derive closed-form expressions for the total number of events k, the time of the k-th event t_k, and a state-space equation linking control parameters to event counts, enabling a direct discrete recurrence formulation. Additionally, a Lyapunov-based stability analysis accounts for exogenous disturbances to guarantee uniform ultimate boundedness (UUB) of the tracking error, providing an explicit design condition for the triggering threshold h in terms of a desired practical precision ϵ. Unlike existing approaches that rely primarily on bounds or linear matrix inequalities (LMI), our method provides direct analytical expressions, enabling predictive co-design of controllers and triggering mechanisms. Simulation results validate the theoretical findings.**

***Index Terms*—event-triggered control, LTI systems, closed-form analysis, Lyapunov stability, monotonic response**

I. Introduction

Event-triggered control (ETC) has emerged as a paradigm for control systems operating under communication and computational constraints. Unlike traditional periodic sampling, ETC updates the control signal only when a predefined event condition is satisfied. This mechanism reduces the number of transmissions while preserving the desired control performance, making it particularly suitable for Networked Control Systems (NCS), Internet of Things (IoT) devices, wireless sensor networks, and distributed robotic systems where communication resources are limited.

In this work, the event-triggering mechanism follows the Send-on-Delta (SoD) policy, where transmissions occur only when the deviation between the current measured state and the last transmitted value exceeds a predefined threshold. Consequently, ETC design often requires iterative tuning of that threshold, evaluating system performance through simulation. While effective, this approach limits the ability to predict communication load and complicates the joint design of control performance and resource utilization.

This paper developed a framework that relates the triggering threshold to the number of generated events. Establishing such a relation provides useful design equations that allow engineers to estimate the expected communication activity of an ETC system before implementation. This capability is particularly valuable for co-design problems, where control performance and communication resources must be considered simultaneously.

Focusing on monotonic LTI systems, we derive analytical expressions for event timing and counts, extending this to general LTI models via a state-space formulation. Our contributions include closed-form communication load estimation, an exact recursive derivation for first-order systems, and a state-space generalization for monotonic dynamics. These results provide a theoretical foundation for predicting communication savings, enabling proactive co-design of control and network resources.

II. Related Work

ETC has been extensively studied regarding stability and resource efficiency. Tabuada [1] established the seminal paradigm of state-dependent triggering, utilizing Lyapunov-based conditions to ensure asymptotic stability. Subsequent research has addressed implementation challenges, such as Zeno behavior avoidance and the guarantee of Minimum Inter-Event Times (MIET) [2], as well as dynamic triggering mechanisms designed to reduce conservatism in threshold selection [3].

State-space formulations have further enabled the co-design of controllers and triggers for NCS under communication constraints [4], [5], while extensions to nonlinear and decentralized systems have focused on deriving explicit bounds for inter-event times [6]. More recent approaches include data-driven methods and multi-agent applications [7], [8].

Despite recent advancements, including data-driven and hybrid system techniques [9], the prevailing literature relies heavily on conservative bounds, numerical optimization, or LMI [10]. Consequently, explicit design equations for predicting communication load remain scarce. Although early works [11], [12] noted an intuitive $k \propto h^{-1}$ scaling rule for monotonic systems, they lacked formal mathematical proofs.

In contrast, this work provides a rigorous framework, deriving exact analytical closed-form expressions for event metrics (including a discrete linear recurrence that is exact under monotonicity). By moving beyond estimation-based bounds and heuristic observations, our framework enables precise communication load prediction and predictive co-design.

III. System Model and Preliminaries

Consider a LTI system described by the state-space equations:

$$\dot{x}(t) = Ax(t) + Bu(t), \qquad (1)$$
$$y(t) = Cx(t),$$

where $x(t) \in \mathbb{R}^n$ is the state vector, $u(t) \in \mathbb{R}^m$ is the input signal, and $y(t) \in \mathbb{R}^p$ is the output, with $A \in \mathbb{R}^{n\times n}$, $B \in \mathbb{R}^{n\times m}$, and $C \in \mathbb{R}^{p\times n}$.

To introduce the event-triggered execution mechanism, let $k \in \mathbb{N}$ denote the event count, and let $t_k \in \mathbb{R}_{>0}$ denote the execution time of the k-th triggered event, which occurs when a triggering condition is satisfied—in this work (8). Over each inter-event interval, a proportional control law can be implemented as

$$u(t) = K_p(w - y(t_k)), \quad t \in [t_k, t_{k+1}), \qquad (2)$$

where $w \in \mathbb{R}$ is a constant reference and $K_p \in \mathbb{R}$ is the proportional gain. Note that while the control signal $u(t)$ is piecewise constant due to the event-triggered mechanism, the state evolution within each interval $t \in [t_k, t_{k+1})$ is governed by the LTI dynamics driven by the constant sample $y(t_k)$.

At the instant an event occurs ($t = t_k$), the loop is momentarily closed with fresh output information, and the true instantaneous dynamics of the system become as

$$\dot{x}(t_k) = (A - BK_pC)x(t_k) + BK_pw = \hat{A}x(t_k) + \hat{B}w, \quad (3)$$

where $\hat{A}$ is assumed Hurwitz. This continuous closed-loop formulation serves as the continuous nominal trajectory upon which our analytical framework is built, abstracting the inter-event deviations.

To establish the closed-form analytical expressions, we first evaluate a first-order system, which serves as a prototype prior to generalizing the framework. Consider the system formulated as

$$\dot{y}(t) = -ay(t) + bu(t), \qquad (4)$$

where a, $b \in \mathbb{R}$ are the system parameters.

IV. Analytical Derivations for the Simple Case

In this section, the inter-event time and the exact total event count are derived. The analysis considers continuous-time systems with strictly monotonic decreasing error responses and no overshoot. Employing (4) and applying a proportional control law $u(t) = K_pe(t)$ under a constant reference w, where $e(t) \in \mathbb{R}$, and defined as $e(t) := w - y(t)$, the closed-loop dynamics is governed by

$$\dot{y}(t) = -(a + bK_p)y(t) + bK_pw. \qquad (5)$$

Solving this differential equation for the zero initial conditions ($y(0) = 0$) yields the output response as

$$y(t) = y_{ss}\left(1 - e^{-\alpha t}\right), \qquad (6)$$

where $y_{ss} = \lim_{t\to\infty} y(t) = \frac{bK_pw}{a+bK_p}$ represents the steady-state output, and $\alpha = a+bK_p$ represents the closed-loop decay rate. Consequently, the error signal $e(t)$ can be formulated as

$$e(t) = e_{ss} + \gamma e^{-\alpha t}, \qquad (7)$$

where $e_{ss} = \lim_{t\to\infty} e(t) = w - y_{ss}$ is the steady-state error, and the transient amplitude is given by $\gamma = y_{ss}$.

A. Event Condition

The SoD triggering condition is defined as

$$|e(t) - e(t_k)| \geq h \qquad (8)$$

where $h \in \mathbb{R}_{>0}$ is the event threshold and $e(t_k)$ is the last measured error transmitted at the previous event time t_k. Thus, an event is triggered when the difference between the current measured error and the last measured error transmitted exceeds a predefined threshold h.

The parameter h sets the triggering mechanism sensitivity. Lower h values increase event frequency, while higher values reduce transmissions at the expense of larger deviations between the current state and the last transmitted value.

Throughout this work, we consider a Single-Input Single-Output (SISO) LTI system, thus $m = p = 1$, which is consistent with the SoD triggering condition defined on a scalar error signal (8).

B. Inter-event Time

The first objective is to determine the time interval between two consecutive events. Let the next event occur at

$$t_{k+1} = t_k + \Delta, \qquad (9)$$

where Δ is the inter-event time to be determined. The triggering condition is satisfied when the error deviation since the last event reaches the threshold. Employing (7) and (9), this leads to

$$|e(t_k) - e(t_k + \Delta)| = \gamma e^{-\alpha t_k}(1 - e^{-\alpha\Delta}) = h. \qquad (10)$$

Solving for the exponential term gives us

$$e^{-\alpha\Delta} = 1 - \frac{h}{\gamma}e^{\alpha t_k}, \qquad (11)$$

which yields the analytical prediction of the next inter-event time

$$\Delta = -\frac{1}{\alpha}\ln\left(1 - \frac{h}{\gamma}e^{\alpha t_k}\right). \qquad (12)$$

This expression predicts the time at which the next event will occur based on the current event time t_k and the system parameters.

C. Closed-form Event Count

The previous expression can be approximated using the Taylor expansion $e^z \approx 1 + z$ for small $z \in \mathbb{R}$, yielding

$$\Delta \approx \frac{h}{\alpha\gamma} e^{\alpha t}. \tag{13}$$

Thus, the corresponding event rate is

$$\frac{dk}{dt} \approx \frac{\alpha\gamma}{h} e^{-\alpha t}. \tag{14}$$

Integrating over time provides the total number of events up to time T as

$$k(T) = \left\lfloor \frac{\gamma(1 - e^{-\alpha T})}{h} \right\rfloor, \tag{15}$$

which represents the closed-form relation between the event threshold and the accumulated number of events. It should be noted that as k denotes a discrete count of events, the result of (15) must use a floor function to ensure $k \in \mathbb{N}$.

For long time horizons,

$$k = \left\lfloor \frac{\gamma}{h} \right\rfloor. \tag{16}$$

This expression reveals that the total number of events is inversely proportional to the event threshold.

D. Recursive Interpretation

An alternative derivation can be obtained without using Taylor approximation. Applying the triggering condition (8) to the transient component leads to

$$\gamma e^{-\alpha t_k} - \gamma e^{-\alpha t_{k+1}} = h. \tag{17}$$

Defining the auxiliary variable $z_k = \gamma e^{-\alpha t_k}$, the triggering condition becomes the linear recurrence $z_{k+1} = z_k - h$.

Solving the recurrence gives us

$$z_k = z_0 - kh = \gamma - kh \quad (t_0 = 0). \tag{18}$$

Substituting back into the exponential form yields the event time expression

$$t_k = -\frac{1}{\alpha} \ln\left(1 - \frac{kh}{\gamma}\right). \tag{19}$$

Isolating k in (19) directly produces (15), confirming the consistency of the analytical derivation.

E. Conditions for Physical Implementation

The logarithm argument must satisfy

$$0 < 1 - \frac{h}{\gamma} e^{\alpha t_k} < 1 \tag{20}$$

to ensure real and positive inter-event times.

From (19) the additional constraint

$$h < \frac{\gamma}{k} \tag{21}$$

must also hold. These conditions prevent non-physical solutions such as negative times or infinite event sequences and define the admissible range of the event threshold for practical implementation.

V. State-Space Generalization

The previous section derived expressions for the event evolution in the simple first-order case. We now extend this result to a general SISO LTI system expressed in state-space form. The objective is to obtain a relation between the event threshold and the number of generated events for systems whose response is monotonic, independently of their order.

To characterize the monotonicity assumption, we recall that a SISO LTI system exhibits a strictly monotonic error response if the time derivative of its tracking error does not change sign for all $t > 0$. A sufficient condition for this property in state-space is that the closed-loop state matrix $\hat{A}$ possesses strictly real and negative eigenvalues (implying an overdamped system response), and the system configuration lacks dominant zeros or non-minimum phase zeros that induce overshoot or undershoot. Under these conditions, the error trajectory $e(t)$ decays monotonically toward its steady-state value.

Consider the closed-loop system with constant reference input w and initial condition $x(0) = 0$. The output response can be written as

$$y(t) = \hat{C}\hat{A}^{-1}(e^{\hat{A}t} - I)\hat{B}w, \tag{22}$$

where $\hat{A}, \hat{B}, \hat{C}$ represent the closed-loop state-space matrices.

Following the definition of the tracking error $e(t) := w - y(t)$, which yields

$$e(t) = w + \hat{C}\hat{A}^{-1}\hat{B}w - \hat{C}\hat{A}^{-1}e^{\hat{A}t}\hat{B}w. \tag{23}$$

An event is triggered when the error variation between two consecutive events reaches the threshold h. Assuming, without loss of generality, a positive step reference $w > 0$, the scalar tracking error $e(t)$ is strictly monotonically decreasing towards its steady-state value ($\dot{e}(t) < 0$). Consequently, $e(t_k) > e(t_{k+1})$ for all k, which guarantees that the error difference is strictly positive. Thus, the absolute value in the triggering condition $|e(t_k) - e(t_{k+1})| = h$ can be safely omitted, yielding

$$e(t_k) - e(t_{k+1}) = h. \tag{24}$$

To evaluate this transition, we define the scalar auxiliary variable

$$z_k = \hat{C}\hat{A}^{-1}e^{\hat{A}t_k}\hat{B}w. \tag{25}$$

Note that for the SISO case, the term $\hat{C}\hat{A}^{-1}e^{\hat{A}t_k}\hat{B}w$ evaluates to a scalar value, which is consistent with the scalar nature of the triggering condition $|e(t_k) - e(t_{k+1})| = h$.

By substituting (23) into (24), the constant terms cancel out, and the discrete event-triggering condition can be expressed in terms of (25) as:

$$\begin{aligned}
(w + \hat{C}\hat{A}^{-1}\hat{B}w - z_k) - (w + \hat{C}\hat{A}^{-1}\hat{B}w - z_{k+1}) &= h \\
z_{k+1} - z_k &= h \\
z_{k+1} &= z_k + h
\end{aligned} \tag{26}$$

Note that (26) holds the discrete event sampling instants t_k due to the sign-preserving nature of the monotonic trajectory. Consequently, we can use this recurrence relation, and solving it yields

$$z_k = z_0 + kh, \tag{27}$$

where the initial value $z_0 = \hat{C}\hat{A}^{-1}\hat{B}w$ is obtained by evaluating (25) at $t_0 = 0$.

Substituting (27) back into the state-space expression yields a relation between the number of events and time

$$k(t) = \left\lfloor \frac{\hat{C}\hat{A}^{-1}(e^{\hat{A}t} - I)\hat{B}w}{h} \right\rfloor \tag{28}$$

This result generalizes the analytical structure obtained for the first-order system to any monotonic LTI system. The number of generated events depends on the closed-loop dynamics through the matrix exponential and remains inversely proportional to the event threshold h. The result of (28) uses a floor function to ensure $k \in \mathbb{N}$.

A fundamental property of the generalized expression (28) is its structural independence from the specific linear control law applied. Let the controller be any linear dynamic compensator (e.g., PID, lead-lag) or static gain (e.g., full state-feedback, LQR, or P control). The closed-loop dynamics can always be formulated in an augmented state-space form such that

$$\dot{\xi}(t) = \hat{A}\xi(t) + \hat{B}w, \quad y(t) = \hat{C}\xi(t), \tag{29}$$

where $\xi(t) = [x(t)^T, x_c(t)^T]^T$ is the augmented state vector containing the plant states $x(t)$ and the dynamic controller states $x_c(t)$.

For instance, if a simple Proportional output-feedback controller with gain K_p is applied, the augmented matrices reduce to the original plant dimensions with $\hat{A} = A - BK_pC$, $\hat{B} = BK_p$, and $\hat{C} = C$, yielding

$$k(t) = \left\lfloor \frac{C(A - BK_pC)^{-1}\left(e^{(A-BK_pC)t} - I\right)BK_pw}{h} \right\rfloor. \tag{30}$$

Consequently, the analytical framework derived herein is applicable to any linear control scheme. As long as the resulting closed-loop matrices $\hat{A}, \hat{B}, \hat{C}$ satisfy the strict monotonicity condition established earlier, the event count prediction remains exact, effectively decoupling the event-generation analysis from the controller synthesis.

VI. Stability Analysis

We derive a practical stability condition using Lyapunov functions, ensuring that the tracking error system is uniformly ultimately bounded (UUB) within a predictable neighborhood of the steady-state equilibrium e_∞, thereby explicitly linking the threshold h to a target precision ϵ. Furthermore, we incorporate an exogenous disturbance term $d(t)$, with $\|d(t)\| \leq \bar{d}$, to account for non-ideal operating conditions and enhance the robustness of the event-management policy.

The event-based execution introduces a state error representation defined as $\delta_x(t) = x(t) - x(t_k)$ for $t \in [t_k, t_{k+1})$. Consequently, the measurement error deviation satisfies $\delta_e(t) = -C\delta_x(t) = e(t) - e(t_k)$, which is strictly bounded by the triggering mechanism such that $\|\delta_e(t)\| \leq h$. Let the steady-state equilibrium be denoted as $x_\infty = -\hat{A}^{-1}\hat{B}w$ and $e_\infty = w - Cx_\infty$, where $\hat{A} = A - BLC$ represents the generalized closed-loop state matrix under the static output feedback control law, with $L \in \mathbb{R}^{m\times p}$ denoting the constant feedback gain matrix. The perturbed closed-loop dynamics, incorporating external disturbances, are formulated as:

$$\dot{x}(t) = \hat{A}x(t) + \hat{B}w + BLC\delta_x(t) + d(t). \tag{31}$$

Theorem 1. *Consider the perturbed closed-loop dynamics subject to an event-triggering mechanism with threshold h and an exogenous disturbance bounded by $\|d(t)\| \leq \bar{d}$ (31). Assume that the output matrix C is full column rank. For a specified maximum allowable steady-state deviation $\|e - e_\infty\| < \epsilon$, the tracking error system is Uniformly Ultimately Bounded (UUB) if the triggering threshold is chosen such that*

$$h < \sigma_{\min}(C)\left(\frac{\epsilon}{\|C\|\sqrt{\frac{2\kappa}{\lambda_{\min}(Q)}}} - \frac{\bar{d}}{\|BLC\|}\right), \tag{32}$$

where $Q = Q^T > 0$, $\lambda_{\min}(Q)$ is its minimum eigenvalue, and κ is a positive constant dependent on the Lyapunov matrix P and the system matrices.

Proof. Defining the state error coordinate as $\tilde{x}(t) = x(t) - x_\infty$, the error system dynamics become

$$\dot{\tilde{x}}(t) = \hat{A}\tilde{x}(t) + BLC\delta_x(t) + d(t). \tag{33}$$

Consider a quadratic Lyapunov candidate function $V = \tilde{x}^T P\tilde{x}$, where $P = P^T > 0$ is the unique positive-definite solution to the continuous-time Lyapunov equation $\hat{A}^T P + P\hat{A} = -Q$ for a given $Q = Q^T > 0$. The time derivative of V along the trajectories of the error system is

$$\dot{V} = -\tilde{x}^T Q\tilde{x} + 2\tilde{x}^T P(BLC\delta_x(t) + d(t)). \tag{34}$$

By applying the properties of matrix norms and Young's inequality, the cross-terms can be upper-bounded as

$$\begin{aligned} |2\tilde{x}^T P(BLC\delta_x + d(t))| \leq \frac{\lambda_{\min}(Q)}{2}\|\tilde{x}\|^2 \\ + \frac{2\|P\|^2}{\lambda_{\min}(Q)}(\|BLC\|\|\delta_x\| + \bar{d})^2, \end{aligned} \tag{35}$$

which leads to

$$\dot{V} \leq -\frac{\lambda_{\min}(Q)}{2}\|\tilde{x}\|^2 + \kappa(\|\delta_x\| + \bar{d}/\|BLC\|)^2, \tag{36}$$

where $\kappa = \frac{2\|P\|^2\|BLC\|^2}{\lambda_{\min}(Q)}$.

To relate the state deviation $\|\delta_x\|$ to the triggering threshold h, we use the assumption that the output matrix C is full column rank (i.e., $\text{rank}(C) = n$), which represents a configuration where the full state vector is reconstructible through the measured channels. Under this geometric formulation, the algebraic property of the minimum singular value dictates that $\|C\delta_x\| \geq \sigma_{\min}(C)\|\delta_x\|$. Since the trigger guarantees $\|C\delta_x\| \leq h$, we can isolate the state deviation bound as

$$\|\delta_x\| \leq \frac{h}{\sigma_{\min}(C)}. \tag{37}$$

Substituting (37) back into (36) yields

$$\dot{V} \leq -\frac{\lambda_{\min}(Q)}{2}\|\tilde{x}\|^2 + \kappa\left(\frac{h}{\sigma_{\min}(C)} + \frac{\bar{d}}{\|BLC\|}\right)^2. \tag{38}$$

It follows that $\dot{V} < 0$ is strictly guaranteed outside the compact residual set defined by

$$\|\tilde{x}\|^2 > \frac{2\kappa\left(\frac{h}{\sigma_{\min}(C)} + \frac{\bar{d}}{\|BLC\|}\right)^2}{\lambda_{\min}(Q)}. \tag{39}$$

According to standard Lyapunov extension theorems, this ensures that the trajectories are Uniformly Ultimately Bounded (UUB). The ultimate bound for the state error norm is

$$\|\tilde{x}\| \leq \sqrt{\frac{2\kappa}{\lambda_{\min}(Q)}}\left(\frac{h}{\sigma_{\min}(C)} + \frac{\bar{d}}{\|BLC\|}\right), \tag{40}$$

which establishes a direct practical tracking error bound in the output space as

$$\|e - e_\infty\| \leq \|C\|\|\tilde{x}\| \leq \|C\|\sqrt{\frac{2\kappa}{\lambda_{\min}(Q)}}\left(\frac{h}{\sigma_{\min}(C)} + \frac{\bar{d}}{\|BLC\|}\right). \tag{41}$$

Enforcing the specified target precision $\|e - e_\infty\| < \epsilon$ implies that

$$\|C\|\sqrt{\frac{2\kappa}{\lambda_{\min}(Q)}}\left(\frac{h}{\sigma_{\min}(C)} + \frac{\bar{d}}{\|BLC\|}\right) < \epsilon. \tag{42}$$

Isolating the triggering threshold h directly yields the design condition presented in (32). ■

This condition enables design trade-offs. The analysis assumes monotonic decrease and full-rank C; extensions to oscillatory systems require additional analysis.

VII. Numerical Validation

To validate the derivations, simulations were conducted for the first-order plant with $K_p = 1$, reference $w = 1$.

Figure 1 shows the empirical fit N vs. h, confirming $N \approx 0.5003h^{-0.9999}$ with high R^2, aligning with theoretical $N = \gamma/h = 0.5/h$ from (15).

To demonstrate the extensibility of the proposed analytical framework, higher-order LTI systems ($n = 2, 3$, and 5) are evaluated. The system matrices were synthesized to ensure strictly real, negative closed-loop eigenvalues, guaranteeing monotonic step responses. Figure 2 illustrates the relationship between the triggering threshold h and the total event count N across these varying complexities. The simulated power-law regressions yield exponents of $\beta_2 = -1.0006$, $\beta_3 = -1.0142$, and $\beta_5 = -1.0703$ for the second, third, and fifth-order systems, respectively. These values are remarkably close to the

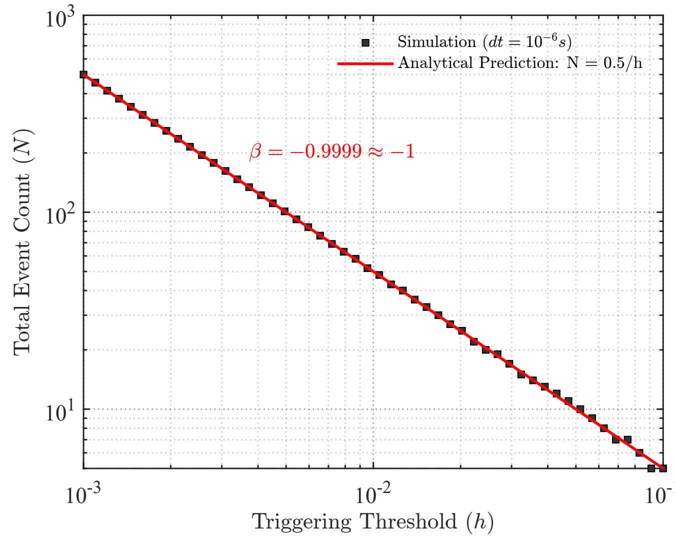

Fig. 1. Total number of events N as a function of the triggering threshold h for the monotonic LTI system $G(s) = \frac{1}{s+1}$. The simulation results (black squares) were obtained using a fixed step size of $dt = 10^{-6}$s to minimize discretization bias. The red line represents the proposed analytical model $k(T) = \frac{\gamma(1-e^{-\alpha T})}{h}$ with $\gamma = 0.5$, $\alpha = 2$ and $T = 10$. The empirical power-law fit $N \propto h^\beta$ yields an exponent $\beta \approx -1$.

theoretical exponent of -1 derived in Section V. Additionally, the simulation markers and solid/dashed prediction lines from (28) in Figure 2 are congruent.

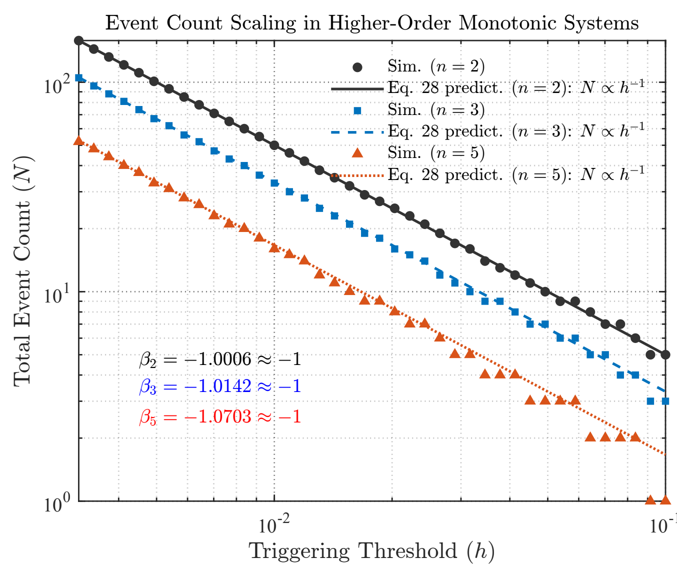

Fig. 2. The log-log plot of the total event count N versus the triggering threshold h for LTI systems of order $n = 2, 3$, and 5. The markers denote simulation results, while the solid/dashed lines represent the analytical prediction derived from (28). The simulated exponents β_n closely match the theoretical value of -1, confirming that the proposed analytical framework is invariant to system order, provided the closed-loop monotonic response condition is maintained.

Finally, Table I compares theoretical k from (28) with simulations for $T = 10$ s and a simulation time step 1×10^{-6} s, showing close agreement.

TABLE I
COMPARISON OF THEORETICAL AND SIMULATED EVENT COUNTS

h	Simulated k	Theoretical k	Error (%)
0.001	500	500	0.0
0.010	50	50	0.0
0.100	5	5	0.0
0.500	1	1	0.0
1.000	0	0	0.0

Note: Theoretical k is obtained by applying the floor function to the value given by Eq. (28).

These results confirm the predictive utility of the closed-form expressions. The close match with simulation data demonstrates that the state-space formulation captures the discrete event-generation process under strict monotonicity.

VIII. DISCUSSION

While the framework provides significant advantages in analytical predictability, several limitations warrant discussion. The assumption of monotonic error decay restricts applicability to systems without overshoot, such as overdamped plants or first-order as analyzed. For oscillatory systems, the recursive method may require modifications to handle absolute values in triggering.

The closed-form expression (28) reveals parametric sensitivity without iterative simulations. Since $k(t)$ is algebraically linked to the closed-loop dynamics, parametric shifts affect event generation proportionally to the transient response (assuming monotonicity). Consequently, the $k \propto h^{-1}$ scaling attenuates parameter mismatch at larger thresholds, offering inherent robustness for predictive co-design.

The implemented SoD mechanism inherently excludes Zeno behavior. Since the state trajectories are continuous and the system dynamics are bounded, the time required for the error signal $|e(t) - e(t_k)|$ to evolve from 0 to a positive threshold $h > 0$ is strictly bounded away from zero [2].

Future extensions may include discretizing for digital implementation ($T_s > 0$). Experimental validation on hardware platforms would further demonstrate practicality.

Compared to literature, our exact formulas complement bound-based approaches [6], offering tools for co-design in resource-constrained environments.

IX. CONCLUSION

This paper introduced a closed-form analytical framework for ETC in monotonic LTI systems, deriving exact expressions for event counts, timings, and threshold design for a wide range of controllers. The framework is characterized by its exact algebraic formulation under the strict monotonicity assumption, and its stability properties, ensuring uniform ultimate boundedness (UUB) under exogenous disturbances via Lyapunov-based analysis. Within this structure, the non-zero threshold policy $h > 0$ directly establishes the physical realizability and operational feasibility of the sampling mechanism. These features, combined with the derived state-space generalizations, provide a powerful set of tools that move beyond conservative bounds toward precise performance co-design.

Although this study focuses on systems with monotonic step responses, the analytical results presented here lay the foundation for a more general theory. Future research will explore the extension of this analysis to oscillating systems, potentially enabling universal event-count prediction for any stable LTI system.

REFERENCES

[1] P. Tabuada, "Event-Triggered Real-Time Scheduling of Stabilizing Control Tasks," IEEE Transactions on Automatic Control, vol. 52, no. 9, pp. 1680-1685, Sept. 2007.

[2] W. P. M. H. Heemels, K. H. Johansson, and P. Tabuada, "An Introduction to Event-Triggered and Self-Triggered Control," 2012 IEEE 51st Annual Conference on Decision and Control (CDC), Maui, HI, USA, 2012, pp. 3270-3285.

[3] A. Girard, "Dynamic Triggering Mechanisms for Event-Triggered Control," IEEE Transactions on Automatic Control, vol. 60, no. 7, pp. 1992-1997, July 2015.

[4] D. Yue, E. Tian, and Q.-L. Han, "A Delay System Method for Designing Event-Triggered Controllers of Networked Control Systems," IEEE Transactions on Automatic Control, vol. 58, no. 2, pp. 475-481, Feb. 2013.

[5] R. Postoyan, P. Tabuada, D. Nešić, and A. Anta, "A Framework for the Event-Triggered Stabilization of Nonlinear Systems," IEEE Transactions on Automatic Control, vol. 60, no. 4, pp. 982-996, April 2015.

[6] P. Tallapragada and N. Chopra, "On Event Triggered Tracking for Nonlinear Systems," IEEE Transactions on Automatic Control, vol. 58, no. 9, pp. 2343-2348, Sept. 2013.

[7] M. Schlüter, M. Nieger, and S. L. J. Michel, "Event-Triggered Learning for Resource-Efficient Networked Control," 2018 Annual American Control Conference (ACC), Milwaukee, WI, USA, 2018, pp. 5036-5041.

[8] T. Liu and J. Huang, "Leader-Following Attitude Consensus of Multiple Rigid Body Systems Subject to Jointly Connected Switching Networks," Automatica, vol. 92, pp. 63-71, June 2018.

[9] W.-L. Qi, R. Wang, M.-S. Yang, Z.-R. Pan, and K.-Z. Liu, "Data-driven dynamic periodic event-triggered control for unknown linear systems: A hybrid system approach," Systems & Control Letters, vol. 199, p. 106067, May 2025.

[10] X.-M. Zhang, Q.-L. Han, X. Ge, D. Ding, B. Ning, and B.-L. Zhang, "An overview of recent advances in event-triggered control," Sci. China Inf. Sci., vol. 68, no. 6, p. 161201, Jun. 2025.

[11] M. Miskowicz, "Event-based sampling with threshold-based trigger," in *Event-Based Control and Signal Processing*, M. Miskowicz, Ed. Boca Raton, FL, USA: CRC Press, 2015, ch. 1.

[12] K. J. Åström, "Event based control," in *Analysis and Design of Nonlinear Control Systems*, A. Astolfi and L. Marconi, Eds. Berlin, Germany: Springer, 2008, pp. 127–147.